Numerical study of Gezon experiment

G Chen, B Roux, D Camel, P Tison, J.P. Garandet, J.J. Favier, A.S. Senchenkov, R Moreau

▶ **To cite this version:**

G Chen, B Roux, D Camel, P Tison, J.P. Garandet, et al.. Numerical study of Gezon experiment. Microgravity Science and Technology, 1994, 7 (2), pp.120-123. hal-01309322

HAL Id: hal-01309322
https://hal.science/hal-01309322

Submitted on 29 Apr 2016

HAL is a multi-disciplinary open access archive for the deposit and dissemination of scientific research documents, whether they are published or not. The documents may come from teaching and research institutions in France or abroad, or from public or private research centers.

L'archive ouverte pluridisciplinaire **HAL**, est destinée au dépôt et à la diffusion de documents scientifiques de niveau recherche, publiés ou non, émanant des établissements d'enseignement et de recherche français ou étrangers, des laboratoires publics ou privés.

Numerical Study of GEZON Experiment

G. Chen, B. Roux, D. Camel, P. Tison, J.P. Garandet
J.J. Favier,A.S. Senchenkov, and R. Moreau

To prepare the microgravity experiment of crystal growth by floating zone method, GEZON, numerical studies of hydrodynamics of the melt are carried out. Calculations of zone length and convection driven by surface-tension gradients are presented for germanium floating zone operating under microgravity conditions. Results of linear stability analysis show the instability of intense thermocapillary convection needed to be damped by using a magnetic field; the critical magnetic induction is obtained. It is expected to grow a striation-free crystal with this magnetic field.

1 Introduction

Since microgravity environment provides the more stable hydrodynamic situations of reduced hydrostatic pressure and buoyancy convection, the floating zone method for the crystal growth has received a great deal of attention as a candidate for use in microgravity [1]. However, stabilization of the molten zone and suppression of buoyancy-driven convection in microgravity is not enough to guarantee the growth of compositionally uniform crystals. Intense thermocapillary convection driven by surface-tension gradients is still present in floating zone, as it has been demonstrated by many researchers; see the references in [2]. In particular, the thermocapillary motion can be intense enough to lead to transition to three-dimensional oscillatory flows which gives striations in the growing crystals [3]. Several techniques have been proposed to control and suppress unsteady thermocapillary convection during processing, such as differential rotation of the feed and the crystal, application of magnetic fields (for electrically conducting fluids), encapsulation and so on.

Because of the very high cost of microgravity experiments, the numerical simulation approach has widely been used to give insight into coupled transport process and to design experimental systems. The present study deals with the preparation of a microgravity experiment, GEZON, prepared to be flown on the *Photon* mission in the *Zona-4* facility. The aim of this experiment is to investigate the influence of the axial magnetic field on the properties of a growing crystal (germanium) by floating zone technique.

Mail address: Dr. Gang Chen, Prof. B. Roux, Institut de Mécanique des Fluids, CNRS UMR 34, 1, rue Honnorat, F-13003 Marseille, France, fax: (33)-91 08 58 91, e-mail: gang@mfmjessy.univ-mrs.fr; D. Camel, P. Tison, J. P. Garandet, J. J. Favier, Service Matériaux et Génie des Procédés, DEM/CENG, 85X, F-38041 Grenoble, France; A. S. Senchenkov, Splav Technical Center, 9, Baikalskaya St., 107497 Moscow, Russia; R. Moreau, MADYLAM/ENSHM, BP95, F-38402 Saint Martin d'Hères, France.

This paper presents the numerical simulation results associated with the GEZON experiment. Sect. 2 describes the calculation of the zone shape and the thermocapillary convection inside the molten zone. This is made of numerical modelling by using NEKTON code. In sect. 3 the linear stability analysis, which combines the numerical solution of an axisymmetric flow with the continuation method, is applied to predict the onset of oscillations. It is shown that for the operating parameters of the GEZON experiment, the thermocapillary convection regime is beyond the predicted stability limit; the flow would be three-dimensional and time-dependent. The stabilizing effect of an axial magnetic field is studied in sect. 4 and the minimum of magnetic induction which should be applied to the experiment is obtained. Finally conclusion is given in sect. 5.

2 Calculation of Zone Length

2.1 Governing Equation

The size of the zone is controlled by the radiative heat transfer between the melt and solid phases with the surrounding ambient and heater, and by the convection in the melt due to surface tension gradients through the shape of the melt. Calculations are based on the configuration as shown in fig. 1. The computational domain consists of three parts: solid feed (left part), the melt (middle part) and crystal (right part). Following assumptions are made in numerical modelling:

(a) axisymmetric model,
(b) absence of gravity, and
(c) flat free surface.

The governing equations are the Navier–Stokes and heat transfer equations in melt (liquid phase):

$$\varrho\left(\frac{\partial \boldsymbol{u}}{\partial t}+\boldsymbol{u}\cdot\nabla\boldsymbol{u}\right)=-\nabla p+\mu\nabla^2\boldsymbol{u}, \tag{1}$$

$$\nabla\cdot\boldsymbol{u}=0, \tag{2}$$

$$\varrho C_p\left(\frac{\partial T_l}{\partial t}+\boldsymbol{u}\cdot\nabla T_l\right)=\kappa_l\nabla^2 T_l, \tag{3}$$

and heat transfer equation in solids

$$\varrho C_p\frac{\partial T_s}{\partial t}=\nabla\cdot(\kappa_s\nabla T_s). \tag{4}$$

2.2 Thermal Boundary Conditions

At the lateral surface, we consider the heat exchange between the sample and the surrounding by radiation

$$-\kappa_i\frac{\partial T}{\partial r}=\varepsilon_i\sigma(T^4-T_a(z)^4),\quad i=l,s, \tag{5}$$

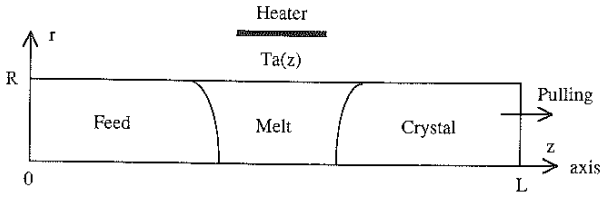

Fig. 1. Configuration of floating zone model and coordinate system

where ε is the emissivity of the sample (liquid or solid) and $T_a(z)$ is the ambient temperature distribution to be imposed in the GEZON experiment along the heater (fig. 2). At the melting/solidifying fronts, thermal boundary conditions are that the energy is conserved across the interfaces and the equilibrium condition

$$\kappa_l \nabla T_l \cdot \boldsymbol{n}_\Gamma - \kappa_s \nabla T_s \cdot \boldsymbol{n}_\Gamma = \varrho \mathscr{L} \frac{\mathrm{d}\Gamma}{\mathrm{d}t}, \tag{6}$$

$$T = T_{melt}, \tag{7}$$

where $\varrho \mathscr{L}$ is the volumetric latent heat of fusion.

At the sample ends, the temperatures are specified

$$z = 0\text{: } T = 953 \text{ K}; \quad z = L\text{: } T = 903 \text{ K}. \tag{8}$$

2.3 Numerical Method

The governing equations are solved numerically using NEKTON [4]. The NEKTON solver is based on a spectral element method which decomposes the computational domain in standard finite element fashion and expands the dependent variables within each element in consistent approximation spaces (N-order Legendre polynomials for the velocity and temperature, and $(N-2)$-order Legendre polynomials for the pressure). The mesh used in the calculations consisted of 24 spectral elements (3 in the radial and 8 in the axial directions) with 10th order Legendre polynomials in each coordinate direction (within each element).

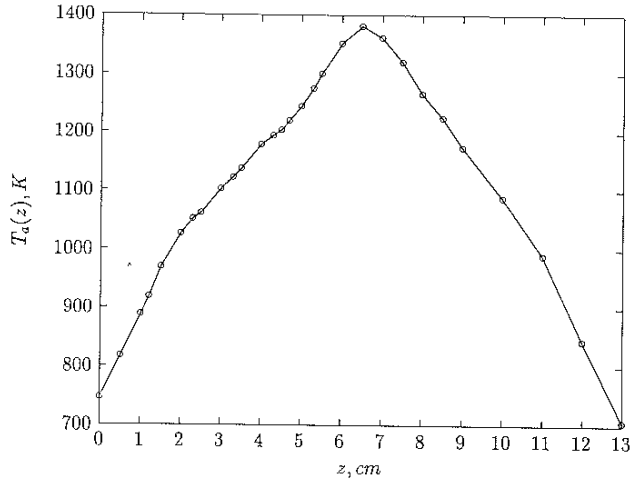

Fig. 2. Temperature distribution along the heater, $T_a(z)$

The accuracy of solutions was verified either by increasing the number of spectral elements or by increasing the order of the Legendre polynomials.

2.4 Results

We present here the flows driven by surface-tension gradients; buoyancy-driven flows are not considered in this work. The thermophysical properties of Ge and the operating parameters used in the calculations are listed in table 1.

Computed zone shape, flow and temperature fields are shown in fig. 3. The flow driven along the surface by surface-tension gradients moves from the hot spot (near the middle of the zone) to the solid surfaces and results in two, axially-stacked toroidal cells (fig. 3b). Because of small Prandtl number of Ge ($Pr = 6 \cdot 10^{-3}$) the isotherms are only slightly deformed from those for a conduction-dominated zone. The calculations demonstrate the asymmetry of flow structure that results from the temperature field asymmetry caused by solidification (or fusion), and by heater temperature distribution used. The melt/solid interfaces are deflected inward showing that the melt is losing heat. Some characteristic results are given in table 2.

Table 1. Thermophysical properties of Ge used in the calculations

sample radius	R	0.75 cm
sample length	L	13 cm
temperature derivative of surface tension	γ	0.105 dyn/(cmK)
thermal conductivity (melt)	κ_l	0.38 W/(cm K)
thermal conductivity (solid)	κ_s	0.18 W/(cm K)
density (melt)	ϱ_l	5.32 g/cm^3
density (solid)	ϱ_s	5.43 g/cm^3
heat capacity	C_p	0.4 J/(gK)
volumetric latent heat of fusion	$\varrho \mathscr{L}$	2,758.44 J/cm^3
melting point temperature	T_{melt}	1,210 K
dynamic viscosity	μ	$5.973 \cdot 10^{-3}$ g/(cm · s)
emissivity (melt)	ε_l	0.18
emissivity (solid)	ε_s	0.5
pulling rate	V_p	$1.4 \cdot 10^{-4}$ cm/s
electrical conductivity	σ_e	$1.52 \cdot 10^4/(\Omega\,\mathrm{cm})$

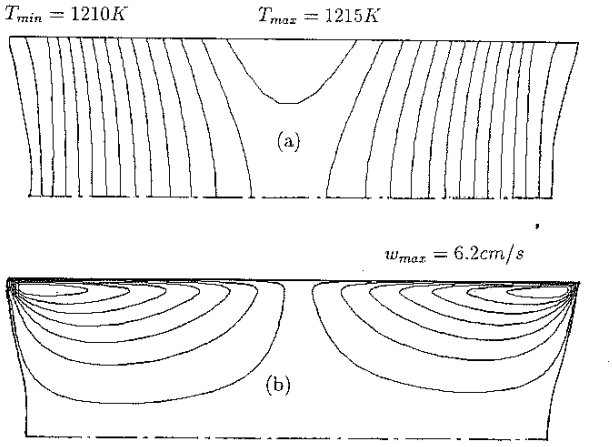

Fig. 3. Numerical axisymmetric solution: (a) temperature field; and (b) stream-function

Table 2. Charcteristic numerical results

temperature difference in the melt	ΔT	5.0 K
maximum velocity at the surface	w_{max}	6.2 cm/s
zone length at the periphery	H_s	2.1 cm
zone length at the axis	H_a	1.9 cm

An appropriate parameter that characterizes the intensity of the surface-tension driven flow is the surface-tension Reynolds number

$$Re = \frac{\gamma \Delta T R}{\mu \nu} = 1.1986 \cdot 10^4 \cdot \Delta T \tag{9}$$

Using the value of ΔT given in table 2 leads to $Re = 5.9929 \cdot 10^4$. We shall show in the following section that the melt flow at this Reynolds number is beyond the stability limit; the flow would be three-dimensional and time-dependent.

3 Linear Stability Analysis

In this section, stability of steady axisymmetric thermocapillary convection is investigated by linear stability theory. Details of the numerical technique employed can be found in an earlier paper [5], only the outline is presented here. A floating zone (liquid bridge) is constructed such that the length of zone is held fixed at $H = (H_s + H_a)/2$ where H_s and H_a are zone lengths at periphery and at axis, respectively. Using the values of H_s and H_a obtained in the previous section (see table 2) gives a floating zone with length $H = 2$ cm, which corresponds to an aspect ratio $A = H/(2R) = 4/3$. The finite difference discretization of governing momentum and energy equations in the floating zone of volume

$$V = \{(r, \theta, z) \mid 0 \le r \le R, 0 \le \theta \le 2\pi, 0 \le z \le H\}$$

yields a system of ordinary differential equations of the form

$$\mathbf{M} \frac{\partial \boldsymbol{x}}{\partial t} + \mathbf{f}(\boldsymbol{x}, T_h) = 0, \tag{10}$$

where $\boldsymbol{x}$ is the solution vector (velocities, pressures, and temperatures), T_h is the maximum temperature of the heater. For certain given T_h, the steady-state solution $\boldsymbol{x}_0$ of eq. (10) (which is assumed to be axisymmetric) will satisfy the equation

$$\mathbf{f}(\boldsymbol{x}_o, T_h) = 0. \tag{11}$$

The linear stability of the steady-state solution $\boldsymbol{x}_o(T_h)$ can be analyzed by taking small perturbations of the form $\xi(r, z)\, e^{-\sigma t + in\theta}$ linearizing in eq. (10) to obtain a generalized eigenvalue problem

$$\mathbf{f}_x \xi = \sigma \mathbf{M} \xi, \tag{12}$$

where n is the azimuthal wave number and $\mathbf{f}_x$ is the discretized Jacobian matrix of the linearized perturbation equations of eq. (10).

As T_h is varied, an axisymmetric steady-state solution may lose stability in one of two ways. One or more generalized eigenvalues of eq. (12) may cross the imaginary axis with zero imaginary part. This case corresponds either to a limit point or to a bifurcation to another steady solution. Alternatively the eigenvalue may cross the imaginary axis at a non-zero imaginary value. This corresponds to a Hopf bifurcation to a periodic solution which is of interest to us. To locate this Hopf bifurcation, we solved an extended steady-state system of equations proposed in [6].

The results of computed critical values (maximum temperature of the heater, corresponding temperature difference in the melt, and Reynolds number) are summarized in table 3 for three azimuthal wave numbers ($n = 0$, 1, and 2). It can be seen that the lowest Re_c corresponds to $n = 1$, showing that three-dimensional disturbances of $n = 1$ are the most dangerous ones.

In the previous section we computed the melt motion and heat transfer in the whole sample using the operating parameters of the experiment, and obtained corresponding experimental Reynolds number, $Re = 5.9929 \cdot 10^4$. Stability analysis presented here revealed that transition of thermocapillary convection from steady-state to oscillation regime occurs at $Re = 8.597 \cdot 10^3$, leading to conclude that the melt motion would be three-dimensional and time-dependent (without magnetic field). However, as it will be demonstrated in the following section, application of an axial magnetic field may stabilize the flow.

4 Effect of Magnetic Field

4.1 Formulation

We use the same physical model as defined in sect. 3 to investigate the influence of an uniform axial magnetic field on the onset of oscillations. The *m*agneto*h*ydro*d*ynamic (MHD) equations that we used in this work are based on the assumptions that the flow field has no influence on the externally applied magnetic field $\boldsymbol{B} = \boldsymbol{B}_o \boldsymbol{e}_z$ while the Lorentz forces are still present. This approximation has been tested and justified in [7] if the magnetic Reynolds number and the magnetic Prandtl number are both small, which is the case in the GEZON experiment. The governing momentum equations for velocity $\boldsymbol{u} = (u, v, w)$ and the equation for the electrical potential ϕ are

$$\varrho\left(\frac{\partial \boldsymbol{u}}{\partial t} + \boldsymbol{u} \cdot \nabla \boldsymbol{u}\right) = -\nabla p + \mu \nabla^2 \boldsymbol{u} + \sigma_e(-\nabla \phi + \boldsymbol{u} \times \boldsymbol{B}) \times \boldsymbol{B}, \tag{13}$$

$$\nabla^2 \phi = \boldsymbol{B} \cdot (\nabla \times \boldsymbol{u}), \tag{14}$$

Table 3. Computed critical values

azimuthal wave number n	temperature of the heater T_h [K]	temperature difference in the melt ΔT [K]	critical Reynolds number Re_c
0	1,257	1.15	$1.3762 \cdot 10^4$
1	1,242	0.72	$8.597 \cdot 10^3$
2	1,249	0.96	$1.1476 \cdot 10^4$

Table 4. Computed critical Reynolds numbers and associated oscillation periods

magnetic induction B_o [mT]	Hartmann number $Ha = B_o R(\sigma_e/\varrho\nu)^{1/2}$	critical Reynolds number Re_c	oscillation period T [s]
0	0	$8.597 \cdot 10^3$	3.96
13	5	$1.0345 \cdot 10^4$	3.83
26	10	$1.5741 \cdot 10^4$	3.52
40	15	$2.8208 \cdot 10^4$	3.01
53	20	$6.2523 \cdot 10^4$	2.28

Equations of conservation of mass and energy are the same as in [5]. The boundary conditions for ϕ are deduced from the assumption that the normal component of the current (j_n) is zero, which implies

$$z = 0, H: \quad \frac{\partial \phi}{\partial z} = 0, \tag{15}$$

$$r = R: \quad -\frac{\partial \phi}{\partial r} + B_o v = 0. \tag{16}$$

4.2 Results

For given magnetic induction B_o, the linear stability analysis presented in sect. 3 is again performed to compute the critical maximum temperature of the heater. Computed critical Reynolds numbers and associated oscillation periods (at the transition) are listed in table 4 for the magnetic induction varying from 0 to 53 mT. The results demonstrate that the presence of an uniform axial magnetic field can stabilize the unstable non-axisymmetric disturbances, thus suppress the thermocapillary instability. With $B_o = 53$ mT we obtain $Re_c = 6.2523 \cdot 10^4$ so that using an axial magnetic induction higher than 53 mT is expected to cause a steady thermocapillary convection in the melt.

In [8] an estimate has been established to consider the dominance of magnetic field effect on the hydrodynamics of the melt; in the first approximation, we got:

$$Ha > Ha_c = Re^{1/3}. \tag{17}$$

In experiments on crystallization of doped germanium samples in the presence of a steady magnetic field carried out on the satellite *Kosmos-1841* the Hartmann number has been found to be 15 while $Ha_c = 34$ (i.e. $Ha < Ha_c$). No significant effect of the magnetic field on macro-nonuniformity has been observed, but it has been found a decrease of micro non-uniformity: 1.9 to 2.5 % without the magnetic field; and 1.1 to 2.1 % with the magnetic field ($Ha = 15$). Also, when taking into account the assumptions used herein, uncertainties of material properties and processing conditions, a magnetic induction of 100 mT has been suggested to be applied in the flight experiment. This corresponds to the estimate of eq. (17).

5 Summary and Conclusion

To prepare the microgravity experiment of crystal growth by floating zone technique, GEZON, we concluded a numerical study of hydrodynamics of the melt. First, the zone shape and the thermocapillary convection applied to GEZON experiment were modelled numerically. The zone length and the maximum of temperature difference in the melt were obtained. The corresponding Reynolds number was found to be $Re = 5.9929 \cdot 10^4$ ($Pr = 6 \cdot 10^{-3}$). A linear stability analysis, which combined the numerical solution of an axisymmetric flow with the continuation method, was then applied to predict the appearance of oscillatory regime. Using the calculated zone length, the critical Reynolds number was determined to be $8.597 \cdot 10^3$, indicating that for the operating parameters of the GEZON experiment, the thermocapillary convection regime is beyond the predicted stability limit; the flow would be three-dimensional and time-dependent. Finally, the effect of an axial magnetic field on the stability of the thermocapillary convection was studied. Application of such magnetic field stabilizes the flow in the melt. When magnetic induction is higher than 53 mT, the computed critical Reynolds number is $6.2523 \cdot 10^4$, which is higher than the experimental Reynolds numbers; the thermocapillary convection will be damped to be steady state. A stronger magnetic induction of 100 mT has been proposed to apply during the flight experiment in order to obtain a striation-free crystal.

Acknowledgements

This work was supported by the Centre National d'Etudes Spatiales (CNES). G. Chen received a Post-Doctoral fellowship from the CNES which is gratefully acknowledged. Computations were performed on the Intel iPSC/860 at the IMFM and IBM3090 of the CNUSC.

References

1 *Brown, R. A.:* Theory of Transport Processes in Single Crystal Growth from the Melt. Journal Review AIChE, vol. 34, p. 881 (1988)

2 *Schwabe, D.:* Surface-tension-driven Flow in Crystal Growth Melts; in: Crystal, vol. 11, *H. C. Freyhardt* (ed.), Springer, Berlin, vol. 11, p. 76–112 (1988)

3 *Eyer, A., Leiste, H., Nitsche, R.:* Floating Zone Growth of Silicon under Microgravity in a Sounding Rocket. J. Crystal Growth, vol. 71, p. 173 (1985)

4 Nektonics, NEKTON User's Guide, version 2.8 (1991)

5 *Chen, G., Roux, B.:* Instability of Thermocapillary Convection in Floating Zone. Proc. 8th European Symp. Materials and Fluid Sciences in Microgravity, ESA SP-333, p. 73 (1992)

6 *Winters, H. K.:* Oscillatory Convection in Liquid Metals in a Horizontal Temperature Gradient. Int. J. Num. Meth. Engng, vol. 25, p. 401 (1988)

7 *Baumgartl, J., Müller, G.:* Calculation of the Effects of Magnetic Field Damping on Fluid Flow – Comparison of Magnetohydrodynamic Models of Different Complexity. Proc. 8th European Symp. Materials and Fluid Sciences in Microgravity, ESA SP-333, p. 161 (1992)

8 *Barmin, I. V., Senchenkov, A. S., Gelfgat, Yu. M., Sorkin, M. Z.:* Thermocapillary Convection in a Magnetic Field. Microgravity sci. technol., vol. 4, p. 76 (1991)